Published by :
http://www.ijert.org

International Journal of Engineering Research & Technology (IJERT)
ISSN: 2278-0181
Vol. 8 Issue 10, October-2019

Design, Fabrication and Testing of Low-Subsonic Open-Circuit Wind Tunnels - A Review

Ishan J. Kelkar
Final Year Diploma Student,
Mechanical Engineering Department,
MAEER's MIT Polytechnic,
Pune, Maharashtra, India

Shreekumar S. Kamalapurkar
Final Year Diploma Student,
Mechanical Engineering Department,
MAEER's MIT Polytechnic,
Pune, Maharashtra, India

Ketan V. Karandikar*
Lecturer,
Mechanical Engineering Department,
MAEER's MIT Polytechnic,
Pune, Maharashtra, India

***Abstract* — A wind tunnel is a device which has a tube-like shape having gradually changing cross-sections like a Venturimeter and having the provision of blowing wind through it with the use of powerful fans. It is a quintessential device for a mechanical and aerospace engineering laboratory to study the behaviour of air-flow around full-sized or scaled-down models of automobiles or aircraft. Thus, it plays a vital role in designing them aerodynamically, saving cost and time incurred in their failure during real-time operation. Small-to-medium sized wind tunnels are used in laboratories for experimental and study purposes. Though these are relatively small in size compared to commercial wind tunnels, meeting their accurate and precise design and fabrication specifications is quite a tough task. This paper deals with the review of several previous researches related to the design, fabrication and testing aspects of such low-subsonic open-circuit wind tunnels. It focuses on design aspects of various wind tunnel components like the test section, contraction cone, diffuser, drive system and the settling chamber. It also sheds light on the materials used for fabricating the same. The results of experimental testing and CFD simulation are also discussed briefly.**

Keywords* — *Circuit, design, fabrication, subsonic, open, review, testing, tunnel, wind.

I. INTRODUCTION

In aerodynamic research, the effects of air flowing past solid objects can be precisely studied by a device called as wind tunnel. It is used to simulate real life wind conditions for aerodynamic analyses of mounted models. It eases the study of fluid analysis, and helps researchers arrive to critical conclusions. It finds its applications in automobile engineering, structural engineering, aeronautics, aerospace, fluid mechanics, aerodynamic analysis of manufactured components like NACA and NREL wind turbine blades, airfoils, spoilers, missiles, drones, Formula 1 racing cars, etc. In many cases related to these applications, theoretical or computational methods alone are not sufficient to obtain precise results, due to either the lack of available equipment, or due to the highly complex nature of the problems taken under consideration. Many a times, the most affordable solution to such scenarios is to test the specimen in a wind tunnel. Testing full or scale models of various components is very popular nowadays. It makes air-flow around an object such that it can simulate real-time flying or forward motion of that object, which can be anything ranging from a small sphere, cuboid, scaled-down model of car to a full-sized aircraft. The air-flow is generated by powerful fans. The motion of air can be studied by employing different methods like generating smoke using a smoke-generating machine or by affixing strings or threads to the object placed inside the wind tunnel. Various parameters of aerodynamics can be measured by using specialized measuring instruments during wind tunnel testing. Modern wind tunnels can simulate the flow regimes which are absent in natural laminar air-flow.

II. HISTORY OF WIND TUNNELS

The early usages of wind tunnels date back to late 19th century which were the early days of aeronautic research. Benjamin Robins invented a whirling arm apparatus to calculate the drag force and performed some experiments related to aviation. Otto Lilienthal employed a rotating arm to measure wing airfoils for various angles of attack to determine lift-to-drag ratio polar diagrams. However, his research lacked the inclusion of induced drag and Reynolds number. The whirling arm was unable to produce a satisfactory wind flow, making the analysis difficult. It was Francis Herbert Wenham, a Council Member of the Aeronautical Society of Great Britain, who found a solution for the problem of faced by the whirling arm and developed the first enclosed wind tunnel in 1871. Konstantin Tsiolkovsky constructed an open-circuit wind tunnel using a centrifugal blower in 1897 and calculated the drag coefficients of flats plates, cylinders and spheres. In 1901, Oliver Wright and Wilbur Wright used a simple open-circuit wind tunnel to analyze the effects of airflow over various shapes while creating their iconic Wright Flyer. It was identified by the Wright Brothers that the effect of air blowing past an aircraft could be simulated by a device. Wind tunnels have evolved greatly from the famous Wright Brothers in 1903 to the modern research facilities funded by NASA. These have greatly shed light on dynamics of fluid and solid objects. When the effect of free stream turbulence on shear

International Journal of Engineering Research & Technology (IJERT)
ISSN: 2278-0181
Vol. 8 Issue 10, October-2019

layers was studied from the year 1930 onwards, design and development of wind tunnels with low levels of turbulence and instability is being stressed upon. Taking this into consideration, closed circuit wind tunnels are being designed due to their characteristic of controlled return flow. These wind tunnels are costly in construction and bulky. Thus, research is being carried out on designing open-circuit wind tunnels which can provide high performance when designed carefully. One of the largest wind tunnels was constructed by the United States in 1941 at Wright Field in Dayton. As of 2019, the world's largest wind tunnel is at NASA Ames National Full-Scale Aerodynamics Complex at Moffett Field, California which has test section dimensions of 80 feet by 120 feet.

III. CLASSIFICATION OF WIND TUNNELS

A. According to Speed:

1) Subsonic Wind Tunnels:

These are the wind tunnels which operate up to Mach 0.75. These are further classified as low and high-subsonic wind tunnels. Low-subsonic wind tunnels are used for testing at very low Mach number, with speeds up to Mach 0.4 (approximately 134 m/s or 495 kmph). These are mainly used for aerodynamic testing of automobiles including passenger cars, racing cars and trucks. High-subsonic wind tunnels are used for testing between Mach 0.4 (approximately 134 m/s or 495 kmph) to Mach 0.75 (approximately 250 m/s or 925 kmph).

2) Transonic Wind Tunnels:

These are the wind tunnels which operate between Mach 0.75 (approximately 250m/s or 925 kmph) and Mach 1.2 (approximately 400 m/s or 1545 kmph). When testing is performed at transonic speeds, additional problems are faced by the researchers. Shock waves generated by the models get reflected and disturb the obtained readings. To minimize this problem, slotted walls are required.

3) Supersonic Wind Tunnels:

These are the wind tunnels which operate between Mach 1.2 (approximately 400 m/s or 1545 kmph) to Mach 5 (approximately 1656 m/s or 6175 kmph). A pre-heating or drying facility is required as the liquefaction of gas can occur due to temperature drop.

4) Hypersonic Wind Tunnels:

These are the wind tunnels which operate between Mach 5 (approximately 1656 m/s or 6175 kmph) and Mach 15 (approximately 4969 m/s or 18522 kmph). It is critical to preheat the nozzle before beginning any test. It is used in the testing of rockets, spacecraft and future space transportation systems.

B. According to Duct Design

1) Open-circuit Wind Tunnels

In this type of duct design, the air from the atmosphere is made to enter the wind tunnel at one end, is passed through it and is then made to flow out back to the atmosphere through the other end. It is also called as Eiffel tunnel named after French civil engineer Compagnie des Etablissements Eiffel or NPL tunnel named after the National Physical Laboratory in England. It consists of four sections from inlet to outlet, namely the settling chamber with honeycomb structure, contraction cone, test section and the diffuser. A fan is either mounted before the contraction cone or at the end of the diffuser. It is widely used for the aerodynamic testing of automobiles like passenger cars, race cars, trucks, etc. It further has two types of designs as follows:

a) Suck-down Type: In this design, the suction-type exhaust fan is located at the end of the diffuser. It is as shown in Fig. 1 below.

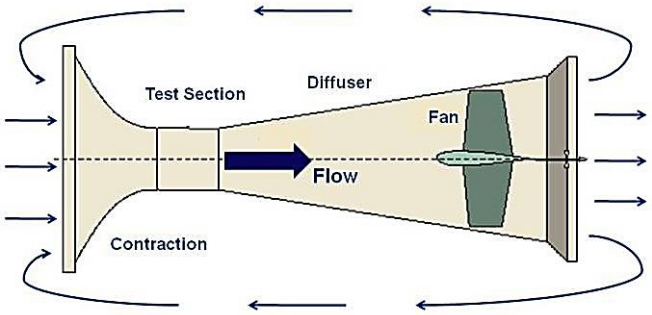

Fig. 1. Suck-down Type Open-circuit Wind Tunnel [1]

b) Blow-down Type: In this design, the blower fan is located at the inlet of the contraction cone.

The main advantage of blower type design over the suck-down type is that it is flexible with respect to the interchanging or modification of test section according to the requirements. It also allows the omission of exit diffuser to allow easy access to the specimen in the test section. However, this results into a considerable loss in power. The suck-down type design is prone to low frequency fluctuations as compared to the blower type. However, this design prevents swirl at the inlet since the suction type exhaust fan is located at the end of the diffuser. This maintains a uniform air flow in the test section. Also, due to the presence of diffuser, the air exits the tunnel smoothly into the atmosphere due to a gradual change in cross-sectional area. [2]

- *Advantages:*

1. Less cost of fabrication as compared to closed-circuit wind tunnels due to simpler construction.
2. During flow visualization using a smoke-generating machine, it does not involve accumulation or purging of smoke since the air and smoke are sent out of the system and fresh air continuously re-enters into the system during operation.
3. It is compact in construction as compared to a closed-circuit wind tunnel.

- *Limitations:*

1. If it is operated in a room, it may need a sufficient sized settling chamber at the inlet in order to achieve high-quality airflow.
2. It may be noisy in operation if it has a cross-sectional area of the test section as large as 70ft^2. This might create problems of noise pollution and may require certain measures to b taken to decrease the noise levels.
3. It requires more energy to operate as compared to a closed-circuit wind tunnel of the same size. However, this can only be a problem for big-sized wind tunnels requiring a high amount of energy to run the blower.

International Journal of Engineering Research & Technology (IJERT)
ISSN: 2278-0181
Vol. 8 Issue 10, October-2019

2) Closed-circuit Wind Tunnels

In this type of duct design, the airflow is recirculated from the exit of the diffuser back to the fan through a series of vanes with minimal or no transfer of air to the atmosphere. It is also called as Prandtl tunnel named after German engineer Ludwig Prandtl or Gottingen tunnel. It is widely used for the aerodynamic testing of aircraft, sports like cycling and in industry where high degree of utilization is involved. It is as shown in Fig.2 below.

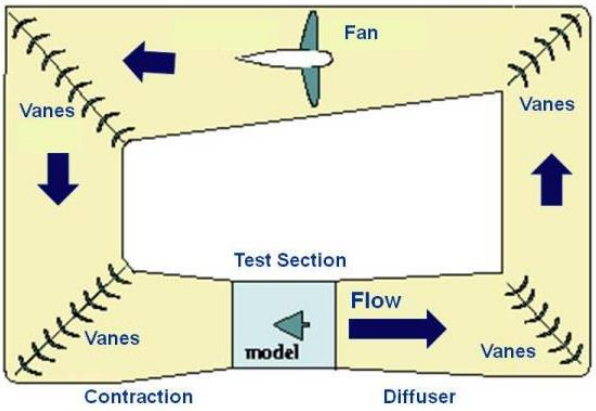

Fig. 2. Closed-circuit Wind Tunnel [1]

- *Advantages:*

1. Since the same air is recirculated in the tunnel, the quality of airflow is maintained at a satisfactory level and it is not affected by any changes in the atmospheric conditions.
2. It requires less energy to operate as compared to an open-circuit wind tunnel of the same size.
3. These wind tunnels are silent in operation as compared to open-circuit ones.

- *Limitations:*

1. More cost of fabrication as compared to open-circuit wind tunnels due to complicated construction.
2. During flow visualization using a smoke-generating machine, there are chances of accumulation of smoke inside the tunnel. This might cause a problem during the analysis of flow parameters.
3. An efficient cooling system may be required if the tunnel has to be operated for longer periods of time.

IV. Measurements Performed by Wind Tunnels

Wind tunnels are used to calculate the following aerodynamic parameters: -

- Drag Force and Co-efficient of Drag (C_D)
- Lift Force and Co-efficient of Lift (C_L)
- Velocity distributions and velocity profiles for various angles of attack
- Pressure distributions and pressure profiles for various angles of attack
- Boundary layers

These parameters prove to be very useful in studying the effects of airflow and determining the stability of different components and models, leading to their most reliable design and efficient performance.

V. DESIGN ASPECTS

A. Test Section:

It is the chamber of a wind tunnel in which the test specimen is mounted and measurements are performed. It is the most important component in any wind tunnel.

It should be designed first depending upon the dimensions of the test specimen and Reynolds number to proceed with the design of the remaining parts of the wind tunnel. The dimensions of the test section should be completely dependent on the testing requirements. The length of the test section must be decided such that the disturbances in air flow resulting from contraction or screens are adequately damped before approaching the test object. However, unnecessarily elongating the test section results in harmful effects – a much larger operating range than that of the selected fan, leads to unsteadiness in flow. The ratio of the length to the diameter of the test section should be more than 1.5. [2]

The blockage ratio of the test section should essentially be less than 10% based on the frontal area of the model. [3]

As a guideline, the test section should generally have a rectangular cross-section with a width-to-height ratio of about 1.4:1.[4]

The design of the test section should be such that it should allow ease of accessibility and installation of the test specimen and measuring instruments. [5]

B. Diffuser:

The core function of the diffuser is to decrease the velocity of the airflow exiting the test section and recovering its static pressure. This reduces the load on the drive system.

The diffuser should have a gradually increasing area from inlet to outlet to avoid flow separation. [6]

Barlow et. al. stated that a conical diffuser should have the divergence half angle less than 3.5° in order to be 'good design.' [3]

A conical diffuser should have an included angle of 5° to have best flow steadiness and the same should be around 10° for best pressure recovery. [7]

The length of the diffuser depends on two variables. The first variable is the diameter or cross-sectional area of the test section and the second variable is the area ratio (AR) of the diffuser section. [8]

The standard AR of the diffuser should be around 3 while keeping an equivalent cone angle of 3^0. [9]

The function of the diffuser is to decelerate the high-speed flow from the test section and to achieve the static pressure recovery. This leads to reduction load on the system. The area of the diffuser should increase gradually along the axis of the wind tunnel to prevent the separation of flow. The divergence half angle of the diffuser walls should be less than 3.5^0 for conical diffusers. They also mentioned that the factors affecting the entrance flow of the diffuser are size or blockage, orientation and wake development of the airfoils. [5]

[21] in their work, added that an ideal Area Ratio (AR) for the diffuser should be between 2 and 5. [10]

C. Contraction Cone:

It is the component of the wind tunnel which is located just after the settling chamber. It serves the purpose of aligning

International Journal of Engineering Research & Technology (IJERT)
ISSN: 2278-0181
Vol. 8 Issue 10, October-2019

and accelerating the air-flow to the desired velocity into the test section.

The quality of the airflow severely depends upon the design of the contraction cone. To keep the boundary layer growth and overall cost of the wind tunnel minimum, the length of the contraction cone should be adequately small. He also stated that it should not be so small that opposing pressure gradients are not formed along the walls of the contraction cone, leading to flow separation. They further stated that the contraction cone should be designed considering the design aspects like entrance height, match point, contraction ratio and overall length. [6]

The optimum contraction ratio should be between 7 and 12. [3]

The contraction sections should be located between the settling chamber and the test section to increase the mean velocity of the air-flow and to reduce the inconsistencies in the air-flow. The contraction ratios must be as large as possible and contraction lengths should be as small as possible to minimize the losses of energy and the boundary layer thickness. Small tunnels should generally have contraction ratios ranging between 4 and 9. Length should be in order of 1.5 times the diameter of the contraction cone. They also itemized that though the past research has shown the importance of a bell-mouthed contraction cone, it is not that critical in the design of small wind tunnels and that a contraction cone having straight walls that form a trapezoid can be considered for the contraction cone design. [2]

A very important point in the design of the contraction section is that the separation of flow in the contraction section can be avoided by making it long, but as the tunnel length is increased, the cost and exit boundary layer thickness also increases. For smaller wind tunnels, a contraction ratio between 6 to 9 should normally be the choice. [11]

D. Drive System Selection:

The drive system can include a fan or blower whose main function is to generate the volume flow-rate of air inside the wind tunnel and also to minimize the pressure losses. The rating of fans is according to the volume flow-rate and static pressure drop which can be overcome by them.

Barlow et.al have included the standard procedure for estimating the losses in the wind tunnel due to the selection of fan. They also detailed that one of the main reasons of background noise is the fan or the drive system. For a wind tunnel with low disturbances, fan noise should be diminished.

A compressor is the best choice for high-speed wind tunnels which require high stagnation pressures. He also specified that centrifugal fans or blowers (push or pull) are the choice of selection for low-speed wind tunnels. [6]

If the diffuser is located at the extreme end of the wind tunnel, an exhaust fan may be used instead of an axial one. [2]

[5] shed light on the types of drive systems that can be used for a wind tunnel. According to them, there are two main types of drive systems viz. compressor and fan. In a compressor, the pressurized air is supplied from storage tanks through a controlling valve to the tunnel. A fan system employs an axial or centrifugal fan or blower of either push-type or pull-type. These can be either shaft-driven or belt-driven. Further, their selection depends upon the available budget and required performance characteristics. Compressors are capable of providing large pressure ratios and they are quite cheap as compared to fans. They are preferred for high-speed wind tunnels requiring high stagnation pressures and for experiments having small testing durations. On the contrary, though fans are expensive, they are best suited for low-speed wind tunnels since they can be used for longer durations of time at once.

[12] found out that even with the use of a large fan, wind speeds remained limited due to significant increase in cross-sectional area.

E. Settling Chamber, Screens and Honeycomb Structure:

Generally, a wind tunnel consists of a honeycomb structure, screens and a settling duct as a part of flow conditioning system. These are located at the before the inlet of the contraction cone.

[13] quoted that a group of screens under tension are placed in the settling chamber. The coarsest screen is located at the entrance and the screens become fine as they reach the test section. This helps in reducing the air turbulence in the test section to a great extent.

[8] in their work, emphasized that the screens in the settling chamber should be spaced at 20 mm apart for making the flow settled before it enters into the second screen. The last screen in the settling chamber should have an open-area ratio of (β) less than 0.57 since the screens with lower ratios tend to produce non –uniformities in the flow. This happens due to the formation of small vortices which are created by the random coalescence of the tiny jet streams coming out of the screens. The pressure drop is dependent on the open-area ratio (β), kinematic viscosity, density and means velocity of the fluid. The formula for calculating the open-area ratio is as given below

$$\beta = \left(1 - \frac{d}{L}\right)^2$$

[11] mentioned that the flow velocity profiles can be made uniform using screens that impose a static pressure drop which is proportional to the square of the air-flow speed. Thus, the boundary layer thickness can be reduced, increasing the ability of the screens to withstand the pressure gradient.

[6] cited that the primary function of the honeycomb structure is to align the air-flow with the axis of the tunnel and to break up the unsteady flow. The screens prevent turbulence in air-flow by cascading the major turbulent fluctuations into smaller ones.

[11] mentioned another important function of honeycomb which is to make the incoming air-flow swirl-free. It also minimizes the lateral variations in the velocity of fluctuations. Generally circular, hexagonal and square-shaped cells collectively form the honeycomb structure. They cited that honeycomb cells have shown the best performance when the length-to-diameter ratio was maintained between 7 and 10. They also specified that the honeycomb should have a thickness of about 6 to 8 times the diameter of each cell.

[3] emphasized on the point that the most suitable shape of cross-section of the honeycomb is hexagonal one, since it has the lowest pressure-drop co-efficient. It also possesses a high structural stiffness to be able to withstand the forces applied without notable deformation.

International Journal of Engineering Research & Technology (IJERT)
ISSN: 2278-0181
Vol. 8 Issue 10, October-2019

[5] highlighted an important fact that the yaw angle for the incoming air-flow should not be more than 10° to prevent stalling of the honeycomb cells. The lowest turbulence in the test section can be achieved by placing multiple screens of different porosities, with the coarsest screen closest to the incoming flow and by placing the finest screen closest to the test section with some free part to decay the fluctuations created by the screen.

[21] tinted that minimum thickness of each cell in the honeycomb structure should be 6.4 cm to lessen the turbulence. Also, the total number of cells should be 150 per settling chamber diameter.

F. Smoke Chamber:

Since air is transparent, to visualize its flow over the test specimen mounted in the test section of the wind tunnel, smoke can be used. For this purpose, a smoke-generation chamber called as the "smoke chamber" is used at the inlet of the wind tunnel, just before the settling chamber.

[3] detailed that the smoke chamber should be located outside or along the wind tunnel.

G. General Guidelines for Design:

[6] suggested that during the design of a wind tunnel, factors like available budget, space and research goals should be considered. Test section size depends upon the Reynolds number in the case of low-speed wind tunnels. Similarly, size of the settling chamber or flow-conditioning section is dependent upon the size of the inlet. Also, design of honeycomb structure decides uniformity of air-flow, screens and succeeding settling chamber length determines the intensity of turbulence in the test section. He also highlighted a very important point of design of low-speed wind tunnel. According to him, the Reynolds number, which is the ratio of inertial forces to viscous forces, plays a very important role in the design. As per his analysis, it is very difficult to achieve Reynolds number similarity even for incompressible flows and increasing the flow velocity assuming air at near-standard conditions is the only method to match the Reynolds number. A wind tunnel which provides a reasonable range of Reynolds number, uniformity in flow and low turbulence intensities can be called as a good quality aerodynamic wind tunnel.

[8] emphasized that there should be a smooth transition between the contraction section and the test section in order to obtain uniform flow in the test section. In order to achieve this, there should be zero slopes at the exit of the contraction section and at the beginning of the test section. Firstly, the velocity that the designer expects to be obtained in the test sections needs to be fixed and depending on this velocity, velocity at any cross-section of the wind tunnel can be found out by using the continuity equation.

VI. FABRICATION ASPECTS

NASA, on their website specifies that the most suitable material for the manufacturing of the contraction cone is 14-gauge sheet metal.

[12] detailed that the manufacturing of settling chamber with the honeycomb structure is quite difficult. They used Aluminium pipes for the honeycomb, taking into account their low weight and high strength. The structure was assembled using nails and the bond between the pipes was made stronger using adhesive glue. The contraction cone was first designed on SolidWorks and constructed using plywood, nails and adhesive. The top and bottom surface of the test section was fabricated of plywood and side surface was fabricated out of fibre glass. Also, the diffuser was constructed out of plywood with dampers to absorb the vibration. Finally, they selected heavy duty fans having large capacity for high speed air velocity. All these components were properly aligned with the help of dampers, nuts and bolts. Also, the leakage of air was checked at each section of joints.

[14] made use of acrylic sheet to make the test section visible, which was bolted to the test section frame. An opening was provided on the front side for easy placement of test models. The contraction cone, settling chamber and diffuser was constructed using Mild Steel plates to reduce costs. Readymade screens were purchased from the local market while honeycomb was made in the laboratory manually using class-A PVC pipes. They revealed the importance of fabricating the diffuser as its one end is rectangular while the other being circular.

[15] in their work, installed two fans which had high efficiency and saved a lot of energy. The motor of the fan was protected using a special hub and the casing and blades of the fan were made up of aluminium which reduced its total weight. A controller unit with a single inverter was used to properly operate the fans. Considering the cost of metal, wood was chosen for the construction of the diffuser. The diffuser section was made up of wood and polycarbonate plates. These are especially light and available in a variety of lengths. The side walls of the test section were made up of Makrolon type of glass with 98% visibility and a thickness of 10 mm. One side of the test section had a window which allowed different types of measurements to be taken on the side of the wind tunnel. The contraction cone was built out of wooden planks and beams. Steel angle brackets and screws were used to attach the various beams. While the planks and beams were connected to each other using flat headed screws, bolts and a special type of glue. Three tables were used to support the entire assembly of the wind tunnel. Such a use of disconnected tables reduced the vibration transfer from the drive section to the test section. All corners were sealed with special tape and extra glue which is used for sealing in ventilation systems. This helped to minimize pressure losses and flow irregularities in the wind tunnel.

[16] constructed the test chamber having a square cross section with 45 degrees chamfer. The diffuser had a length of 332 mm with an expansion angle of 4°. The honeycomb was 3D printed and made up of PLA. A commercially available fan was chosen.

VII. DETAILED LITERATURE REVIEW

[8] Arslanian et.al. (2012), in their work of building solid model of a subsonic wind tunnel for laboratory instructional purposes through CFD simulation assigned a uniform cross-sectional area (A_3) to the octagonal test section of the wind tunnel to reduce the effect of flow eddies, whereas its length was decided according to the design needs. His design was in three phases. In phase 1, length of the diffuser nozzle was

International Journal of Engineering Research & Technology (IJERT)
ISSN: 2278-0181
Vol. 8 Issue 10, October-2019

calculated. The diffuser nozzle length is dependent on two variables, viz. diameter of the test section and the Area Ratio (AR) of the diffuser nozzle. The typical AR should be kept around 3 with the cone angle of 3°. Since A3 was known, area of the diffuser nozzle exit (A4) was found out by using the following equation

$$AR = \frac{A_4}{A_3} = 3 \qquad (1)$$

Radius of the octagonal test section was found out using the following equation

$$A_3 = 8tan\frac{\pi}{8}R_3^2 \qquad (2)$$

The overall dimensions of the wind tunnel are as shown in Fig. 3 below.

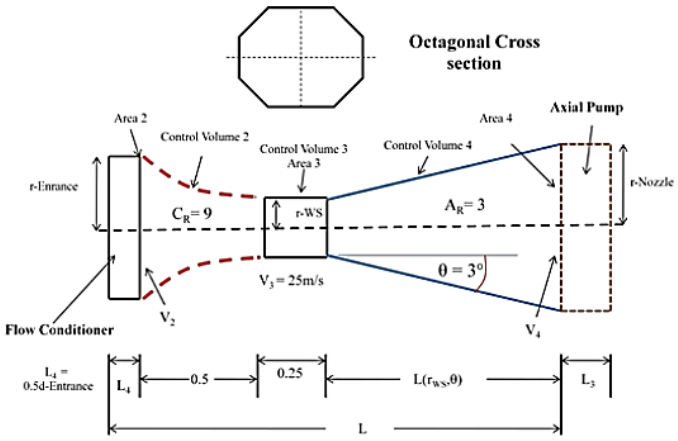

Fig. 3. Overall Dimensions of Wind Tunnel

The geometry of the diffuser is as shown in Fig. 4 below.

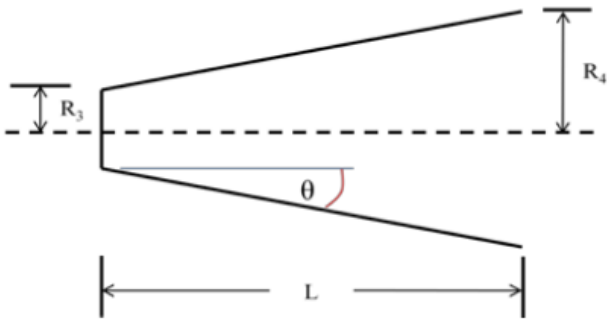

Fig. 4. Geometry of Diffuser

Area of the diffuser nozzle at the exit (A_4) was determined combining equations (1) and (2). Since A_4 was circular, its radius was then calculated by using the following equation

$$R_4 = \sqrt{\frac{A_4}{\pi}} \qquad (3)$$

Finally, length of the diffuser was determined using the following equation and phase 1 was complete.

$$L = \frac{R_4 - R_3}{tan\theta} \qquad (4)$$

An octagonal cross-section was used for the contraction nozzle throughout its length. A Contraction Ratio (CR) of 9 was used for the design of the contraction nozzle. A_2 was calculated using the following equation

$$CR = \frac{A_2}{A_3} \qquad (6)$$

Before proceeding to the next phase, the radius of the contraction nozzle entrance (R_2) was determined using equations (5) and (7) as follows.

$$A_2 = 8tan\frac{\pi}{8}R_2^2 \qquad (5)$$

$$R_2 = \sqrt{\frac{A_2}{8tan\frac{\pi}{8}}} \qquad (7)$$

In phase 2, the fluid flow was evaluated assuming an incompressible, steady and two-dimensional flow with negligible frictional forces to aid the selection of the pump within the budget. The velocity in the test section was set to 25m/s. Since the test section shared common inlet and outlet with the contraction nozzle and the diffuser nozzle respectively, the velocities at different section were determined using the Continuity equation as follows

Velocities at the entrance of the contraction nozzle (U_2) and that at the exit of the diffuser nozzle (U_4) were calculated using equations (8) and (9) as follows.

$$U_2 = \frac{U_3 A_3}{A_2} \qquad (8)$$

$$U_4 = \frac{U_3 A_3}{A_4} \qquad (9)$$

Based on the flow assumptions, Bernoulli's theorem was used to determine the pressures at various sections throughout the tunnel. The ambient velocity (U_1) before the contraction nozzle entrance was assumed to be zero and that point was considered as the stagnation point. Pressures were calculated using equations (10), (11), (12) and (13) as follows.

$$P_{static1} = P_{ambient} = 101.325kPa = P_{stag1} \qquad (10)$$

Pressure at the entrance to the contraction nozzle ($P_{static2}$), pressure in the test section ($P_{static3}$), pressure at the diffuser exit ($P_{static4}$) were calculated using the following equations

$$P_{static2} = P_{stag1} - \rho\frac{U_2^2}{2} \qquad (11)$$

$$P_{static3} = P_{stag1} - \rho\frac{U_3^2}{2} \qquad (12)$$

$$P_{static4} = P_{stag1} - \rho\frac{U_4^2}{2} \qquad (13)$$

Since the pressures at both sides of the pump were known, the pressure recovery provided by the pump was calculated. The fluid pump having the following specifications was selected based on the Volume Flow Rate (VFR) and diameter of the diffuser nozzle

VFR = 683.345 Cubic feet per minutes
ΔP_r = 0.16703 Column inches of water
Diameter = 8.52 in

Design phase 3 was sub-divided into two phases (3-1), (3-2) and (3-3). In phase 3-1, the contraction nozzle contour was designed. The main criterion for the design of the contraction

International Journal of Engineering Research & Technology (IJERT)
ISSN: 2278-0181
Vol. 8 Issue 10, October-2019

contour was that the velocity of the fluid flow at the exit of the contraction nozzle should be uniform. A smooth transition of the contraction contour from the entrance of the contraction nozzle to the entrance of the test section was obtained. The slope at the entrance of the contraction nozzle was required to be zero. The contraction nozzle contour was formed by developing a mathematical model and connecting two cubic arcs at the inflection point as shown in Fig. 5 below.

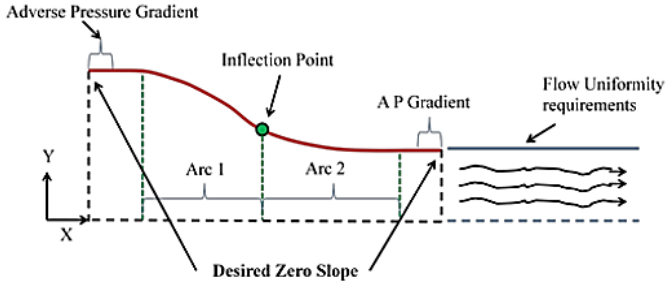

Fig. 5. Contraction Nozzle Contour

In phase 3-2, pressure losses at different sections which were needed to be balanced by the fluid pump were calculated by using equations (18) and (19) as follows.

$$h_l = K\frac{V^2}{2g} = \frac{\Delta P}{\rho g} \qquad (18)$$

$$\Delta P = K\frac{V^2}{2}\rho \qquad (19)$$

where K is the loss coefficient, V is the average fluid velocity, and ρ is the fluid density. In general, the loss coefficient K is a function of friction factor and the geometry of the section.

The axial fan details are as shown in Fig. 6 below.

Section Losses + Pressure recovery = Axial Fan Requirements

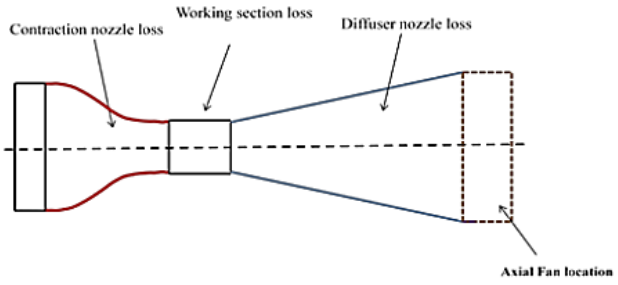

Fig. 6. Axial Fan Requirements

The loss coefficient of the working section was calculated as using equations (20), (21) and (22) as follows.

$$K_{ws} = f_{ws}\frac{L_{ws}}{D_{ws}} \qquad (20)$$

where fws, Lws and Dws are the friction factor, length and the hydraulic diameter of the working section, respectively. The friction factor was calculated using the Colebrook equation, equation (21) as follows.

$$\frac{1}{\sqrt{f}} = -2log_{10}\left(\frac{\varepsilon/D}{3.7} + \frac{2.51}{Re\sqrt{f}}\right) \qquad (21)$$

Assuming zero roughness (ε=0) in the interior of the working section, the Colebrook equation was simplified to equation (22) as follows.

$$\frac{1}{\sqrt{f}} = 2log_{10}\left(Re\sqrt{f}\right) - 0.8 \qquad (22)$$

where Re is Reynolds number

$$Re = \frac{\rho V_{avg} D}{\mu} \qquad (23)$$

where ρ and μ are the density and viscosity of the flow, respectively. $Vavg$ is the fluid average velocity in the working section, which was set at 25m/s by design.

Since the geometry of the test section was known, the hydraulic diameter was calculated using the following equation

$$D = \frac{4A_C}{Per} \qquad (24)$$

where AC is the cross-sectional area, and Per is the wetted perimeter

After this step, the Re was calculated by using equations 22 and 23. Subsequently, the friction factor was calculated and finally the pressure loss in the working section was calculated using equation 19. Based on the total pressure loss, the pressure recovery required by the fluid pump was calculated and a cost-effective pump having the following specifications was selected.

VFR = 683.345 Cubic feet per minutes
ΔP = 0.38828 Column inches of water
Diameter = 8.52 in

Finally, in testing phase 3-3, the flow was evaluated using CFD simulation. A solid model of the wind tunnel was built using SolidWorks 2010 software as shown in Fig. 7 below.

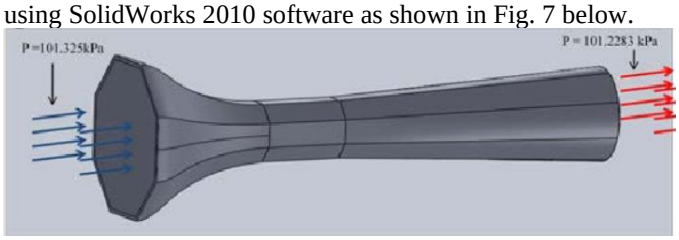

Fig. 7. Solid Model of Wind Tunnel

This model was analyzed for any cross-flow using a FEA simulation software. Fig. 8 below shows the cross-flow and up-flow.

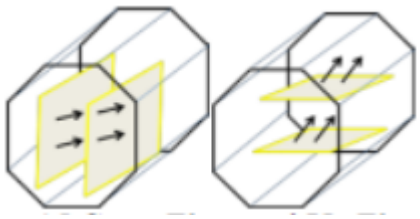

Fig. 8. Cross-flow and Up-flow

Both, the cross-flow and up-flow were obtained in negligible amounts which was a good sign. Prior to inserting a model in the test section, the blockage ratio (which should be less than 7.5%) was calculated by using the following equation

International Journal of Engineering Research & Technology (IJERT)
ISSN: 2278-0181
Vol. 8 Issue 10, October-2019

$$BR = \frac{100}{A_{working\ section}}[A_{model}(model\ scale)^2]$$

A model of a sphere was placed in the test section with a blockage ratio of 6.6% and the velocities around it were studied. According to the simulation, high velocity regions constituted the top and bottom of the sphere while low velocity region was on the left-hand side of it. This conformed well with the theory. The velocity around the sphere is as shown in Fig. 9 below.

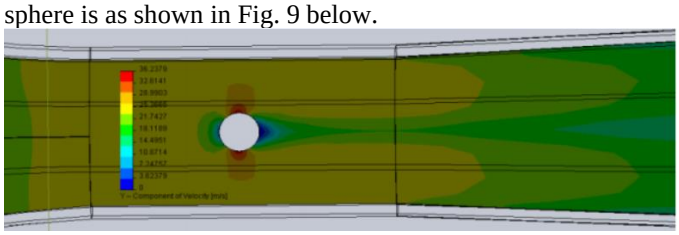

Fig. 9. Simulation of Air-flow around a Sphere

Similarly, a NACA 2412 airfoil was analyzed using simulation software with a blockage ratio of 1.2%. The angles of attack were varied between 0° and 12°. Low-pressure areas were formed on the top of the airfoil while high-pressure areas were formed on its bottom as shown in Fig. 10 below.

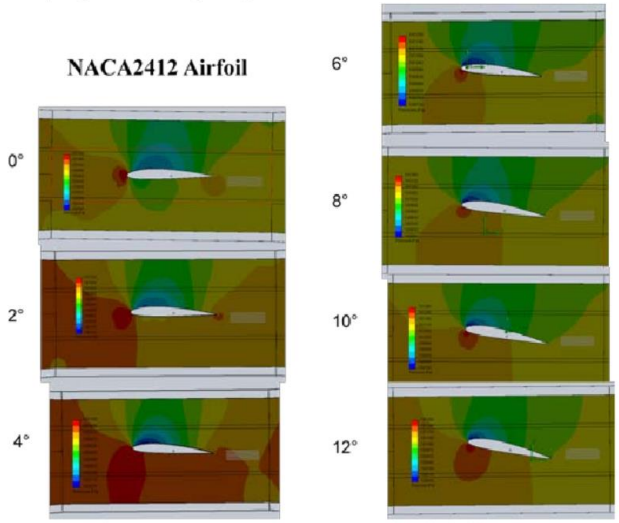

Fig. 10. Simulation of Pressure around NACA 2412 Airfoil

These results obtained were compared with the theoretical ones obtained from MATLAB software and gave a good agreement with them.

Mansi Singh et. al. [2] in their project work of constructing an open-circuit low speed wind tunnel for testing a NACA airfoil initially selected the suitable co-ordinates of standard NACA 63-215 airfoil to best fit their test section dimensions as follows.

Length = 20 cm

Width = 30 cm

Followed by this, they created a model of the airfoil using 3-D modelling software using these co-ordinates as shown in Fig. 11 below.

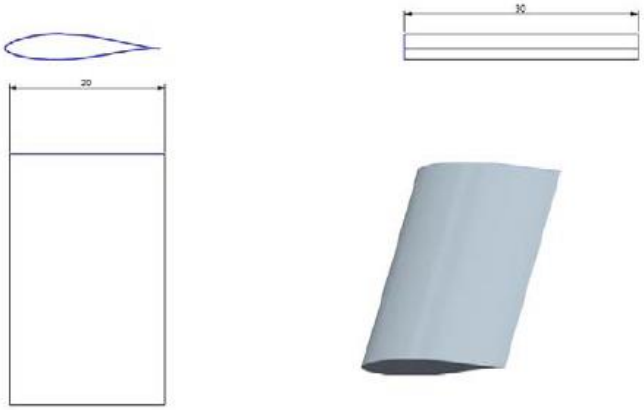

Fig. 11. 3-D Model of NACA 63-215 Airfoil

A test section was designed by taking reference of the dimensions of the airfoil as follows

Cross-section of the test section = 30 cm X 30 cm

Length = diameter (d) X 1.5 = 45 cm

They chose a length as 50 cm (which is greater than 45 cm)

Its CAD model is as shown in Fig. 12 below.

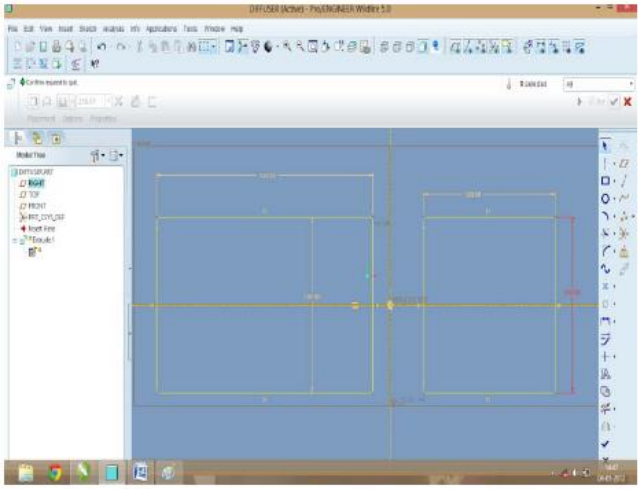

Fig. 12. CAD Model of Test Section

The contraction cone was designed by choosing the contraction ratio as 4, as follows

Contraction ratio = (60 X 60) / (30 X 30) = 4

Cross-section = 60 X 60 cm (for outer end) and 30 X 30 cm (for inner end)

Length of the contraction cone = 1.5 X D = 1.5 X 60 = 90 cm

The CAD model of the contraction cone is as shown in Fig. 13 below.

International Journal of Engineering Research & Technology (IJERT)
ISSN: 2278-0181
Vol. 8 Issue 10, October-2019

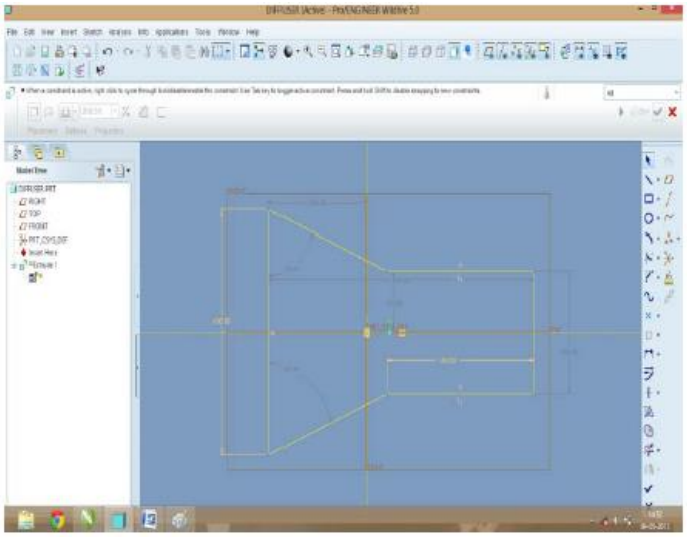

Fig. 13. CAD Model of Contraction Cone

The honeycomb was designed following the dimensions of the contraction cone as follows
Cross section = 60 X 60 cm
Length = 10 cm (to minimize the turbulence)
Its CAD model is as shown in Fig. 14 below.

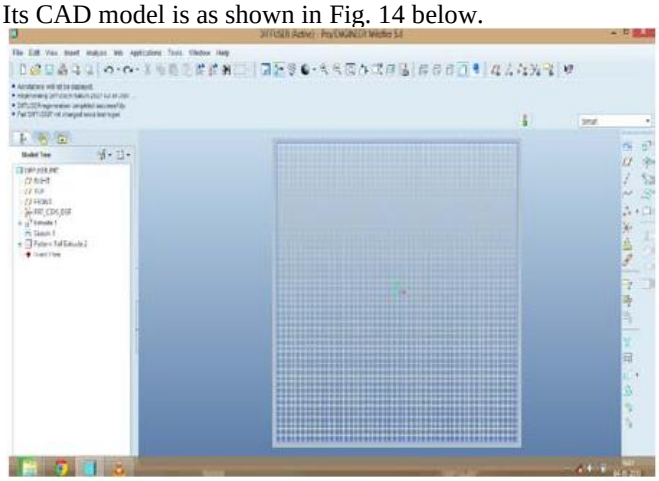

Fig. 14. CAD Model of Honeycomb

The settling chamber was designed following the dimensions of the honeycomb structure and hence its dimensions were similar to it. Its CAD model is as shown in Fig. 15 below.

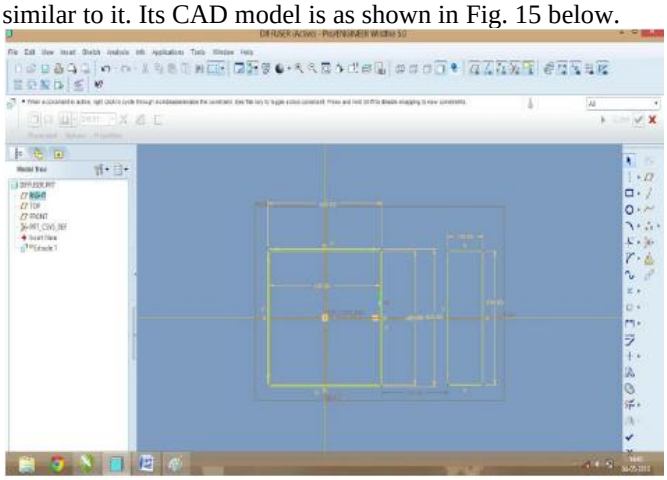

Fig. 15. CAD Model of Honeycomb

The diffuser was designed considering the diffuser angle of the diffuser cone. It was designed such that the angle of diffusion (φ) around 5°. Its calculations are as follows

Half angle of diffusion = φ/2 = 2.54

Thus, the outer diameter (Do) of the diffuser was calculated as follows

$$D_o = D_i + \{2 \text{ X } (L_d \text{ X } \tan \varphi/2)\}$$

where,
D_i = inner diameter of the diffuser = diameter of the test section = 30 cm
L_d – length of the diffuser = 90 cm

Hence, $D_o = 30 + \{2 \text{ X } 90 \text{ X } \tan 2.54\}$

$D_o = 30 + 7.984 = 38$ cm (approx.)

Its CAD model is as shown in Fig. 16 below.

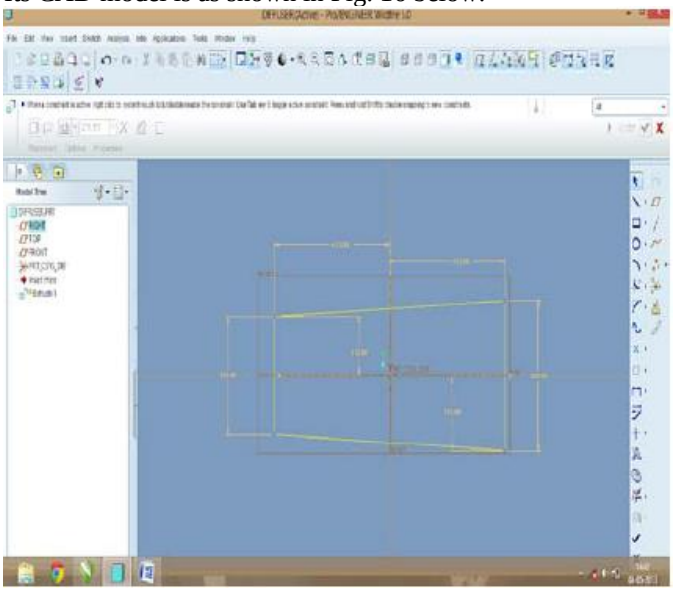

Fig. 16. CAD Model of Diffuser

Since the diffuser was located at the extreme end, hence an exhaust fan of ½ HP giving a velocity of 10 m/s was selected instead of an axial fan.
This completed the design procedure of their wind tunnel and the final specifications were obtained as shown in Fig. 17 below.

Overall length – 10ft
Test Section Length – 50 cm
Test Section Diameter – 30cm
Settling Chamber Diameter – 60cm
Contraction Ratio – 4
Honeycomb Thickness/Cell Size/Cell Count – 10cm
Max Mean Air Velocity – 5.7 m/s
Max Mean output- 4.024 m/s
Diffuser angle- 2.54º

Fig. 17. Specifications of Wind Tunnel

Considering these dimensions, the wind tunnel was fabricated in stages. In stage 1, the contraction cone and diffuser was fabricated using 28 gauge sheet metal since it was easier to bend than the recommended 14 gauge sheet metal. They also verified some designs made up of paper prior to the actual fabrication. The fabricated contraction cone is as shown in Fig. 18 below.

International Journal of Engineering Research & Technology (IJERT)
ISSN: 2278-0181
Vol. 8 Issue 10, October-2019

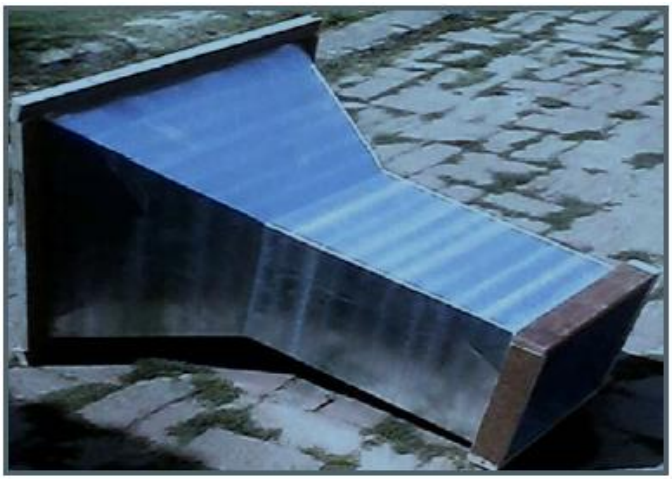

Fig. 18. Fabricated Contraction Cone

During the fabrication of the contraction cone, a problem was faced in using welding as the joining process of the two sections since it cannot be used for GI sheet metal. Hence, they chose to pin the sections at the edges at a sheet metal shop. A frame made up of wood ply having a thickness of 2 cm was nailed at the two ends of the contraction cone. In the next stage, the honeycomb structure was manufactured by using 9260 straws having a diameter of 3 mm and a length of 9 cm. These straws were affixed inside a wooden frame. Finally, considering three sections, the total number of straw pieces was 27800. The cross-section view of the straws is as shown in Fig. 19 below.

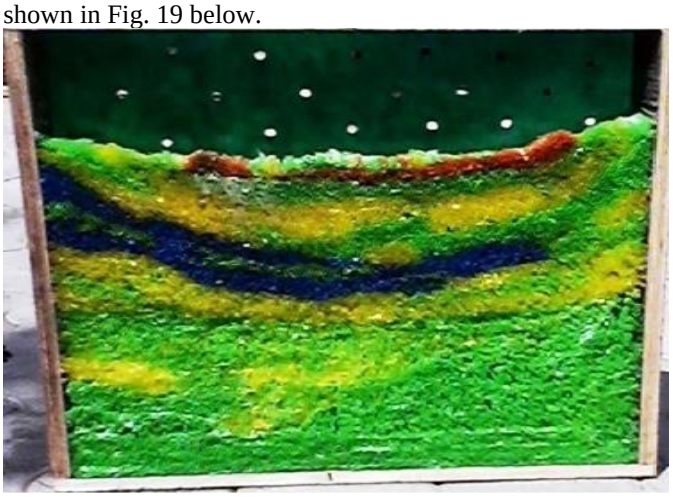

Fig. 19. Cross-sectional View of Straws of Honeycomb

After this, the settling chamber screens were fabricated by using three different sieves having specifications as follows
Outermost sieve with M = 1.5 (Refer Fig. 20)
Middle sieve with M = 9 (Refer Fig. 21)
Innermost sieve with M = 16 (Refer Fig. 22)
(where M = Holes / inch)

Fig. 20. Outermost Sieve (M=1.5)

Fig. 21. Middle Sieve (M = 9)

Fig. 22. Innermost Sieve (M = 16)

After manufacturing the honeycomb, the test section was fabricated using two wooden frames (one at each end) and transparent four Plexiglass panels of thickness 1 mm in between. It is as shown in Fig. 23 below.

International Journal of Engineering Research & Technology (IJERT)
ISSN: 2278-0181
Vol. 8 Issue 10, October-2019

Fig. 23. Fabricated Test Section

To accommodate the rod holding the airfoil to be tested aerodynamically, pitot tube and manometer, holes of diameter 10 mm were drilled in the test section. Finally, a domestic strength fan of 15 inches shroud having two speed levels viz. high and low was attached to the extreme end of the diffuser. The airspeed obtained was between 0 m/s to 20 m/s. The completely fabricated wind tunnel is as shown in Fig. 24 below.

Fig. 24. Completely Fabricated Wind Tunnel

The pressure heads (h) and velocities (v) were obtained as shown in Table I below.

TABLE I. READINGS OF PRESSURE HEAD AND VELOCITY

Sections	Settling Chamber	Test Section	Diffuser
x (mm)	0.8	2	1
h (m) calculated	0.66055	1.650892	0.825
v (m/s) calculated	3.599	5.69122	4.024

The results obtained for lift and drag co-efficient for the test section considering a velocity of 5.7 m/s were as follows: -

Co-efficient of Lift (C_L) = 1.30634

Co-efficient of Drag (C_D) = 6.14588

The velocity profile obtained is as shown in Fig. 25 below.

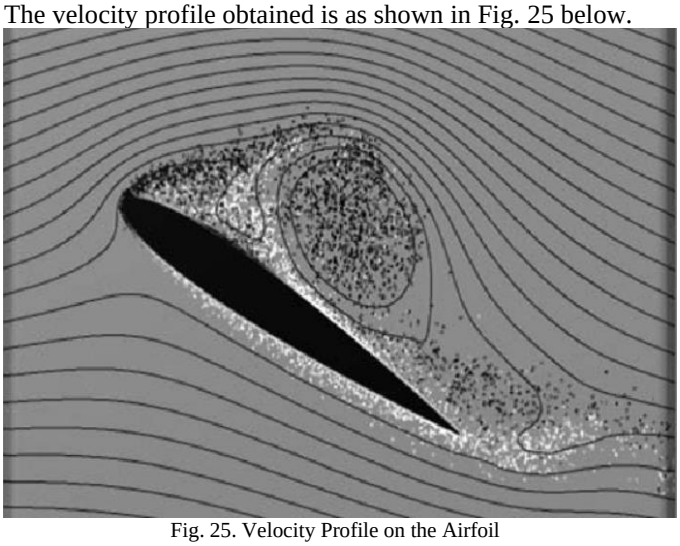

Fig. 25. Velocity Profile on the Airfoil

Smoke was used to visualize the air-flow. After testing five different methods of creating smoke viz. strings, incense sticks, mineral oil, smoke-in-a-can and dry ice, the most successful method was the dry ice one. The airfoil which was tested was remotely controlled for understanding what exactly happens on an aircraft when air passes over a wing. The final conclusions drawn were as follows: -

- The velocity profile as shown in Fig. 25 above shows that the smoke flowing inside the test section has high turbulence.
- A velocity of more than 10 m/s is required to show the effect of velocity on the airfoil.
- The wind tunnel is suitable to test airfoils having a weight of less than 0.15 kg.
- Aerodynamics of any high-speed car or airplane can be studied using this wind tunnel using scaled-down models of the same.

[17] Yong et. al. (2015), in their project work, fabricated a cost-effective wind tunnel in order to conduct small-scale experiments to visualize flow passing through fundamental objects for educational purpose. This wind tunnel mainly focused on testing any scaled-down model, which provided had a width based on Reynolds number of the order of hundred thousand at approximately 5% blockage based on the frontal area. A fourth to sixteenth times scale was deemed adequate for investigations of the underlying flow mechanisms and for basic research and study on simplified bluff and quasi-streamlined bodies. Turbulence intensity of less than 5% at a working speed of 6 m/s to 8 m/s was considered reasonable for testing without compromising the integrity of the results. All these parameters were considered by the researchers, working upon a budget of RM 1500 (approximately INR 30,000). A fan of 150 V was used to generate air velocities in the wind tunnel. The overall dimensions of the wind tunnel are as tabulated in Table II below.

International Journal of Engineering Research & Technology (IJERT)
ISSN: 2278-0181
Vol. 8 Issue 10, October-2019

TABLE II. OVERALL DIMENSIONS OF WIND TUNNEL

Module	Width (m)	Height (m)	Length (m)	Area (m^2)	Area Ratio
Contraction Cone	0.81	0.81	0.610	0.656	7.28
Working Section	0.30	0.30	0.610	0.090	-
Diffuser	0.43	0.43	1.218	0.185	2.05

The material used for fabrication was wood as it was more cost effective than fibre glass or sheet metal. The handling and fabrication were relatively easy as wood is easier to handle. 0.9 cm plywood was used as it was universal and easily available. The test section was made up of Plexi glass in order for it to be transparent. It is as shown in Fig. 26 below.

Fig. 26. Plexi Glass Test Section

For the contraction cone made up of wood, a contraction ratio of 7.28 was selected citing a previous reference. While manufacturing, the gaps between joints were filled using silicone glue to fortify the structure and reduce exfiltration as shown in Fig. 27 below.

Fig. 27. Filling of gaps using Silicone Glue

Rubber gaskets were used in the ends connecting the contraction cone to the test section and the test section to the diffuser to prevent leakage of air. It is as shown in Fig. 28 below.

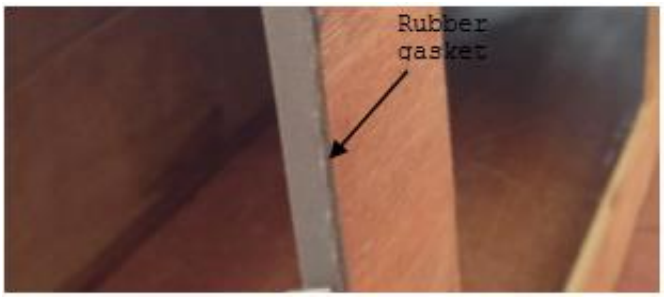

Fig. 28. Use of Rubber Gasket to connect Diffuser

The initial plan of using 1.2 cm diameter straws for constructing the honeycomb structure was cancelled owing to its high construction time. Hence, a wire mesh having 0.5 cm diameter was used as a substitute. It was attached to the contraction cone with the help of stapler bullet. The researchers revealed an important point that the performance of such a honeycomb as shown in Fig. 29 below would be greatly affected adversely since it had no depth.

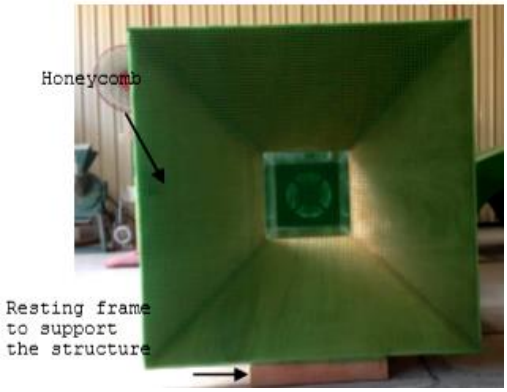

Fig. 29. Honeycomb Structure

According to the researchers, for a suck-down type wind tunnel, the diffuser is the component of least importance since it is located at the downstream of the test section. A diffuser with a trapezium shape as shown in Fig. 30 below was constructed having a slightly larger exit than the entrance and an area ratio of 2.05.

Fig.30. Trapezium-shaped Diffuser

Finally, the contraction cone, test section and the diffuser were assembled together with the use of a frame as shown in Fig. 31 below.

International Journal of Engineering Research & Technology (IJERT)
ISSN: 2278-0181
Vol. 8 Issue 10, October-2019

Fig.31. Supporting Frame

The completed wind tunnel model is as shown in Fig. 32 below.

Fig.32. Completed Wind Tunnel Model

After the completion of manufacturing, the wind tunnel was tested using a simple air-flow anemometer with a data logger having RC-232C interface to detect the incoming wind speed. The turbulence intensity was calculated by using the following equation

$$Tu = \frac{\sqrt{u^2}}{u_{mean}}$$

Keeping a goal of achieving the turbulence intensity within 5%, the anemometer was placed at two different positions in the test section in the boundary layer region as shown in Fig. 33 below.

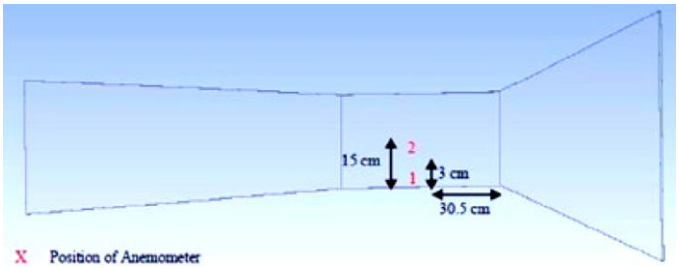

Fig.33. Locations of Anemometers

Experiments were performed according to three different conditions as shown in Table III below.

TABLE III. CONDITIONS FOR TESTING

Experiments	Conditions	Positions (see figure10 for picture illustration)
1	Right after the fan was initiated	1
2	10 minutes after the fan was operated	1
3	10 minutes after the fan was operated	2

Results of velocity with respect to time were obtained and recorded for each experiment and graphs were plotted as shown in Fig. 34 below.

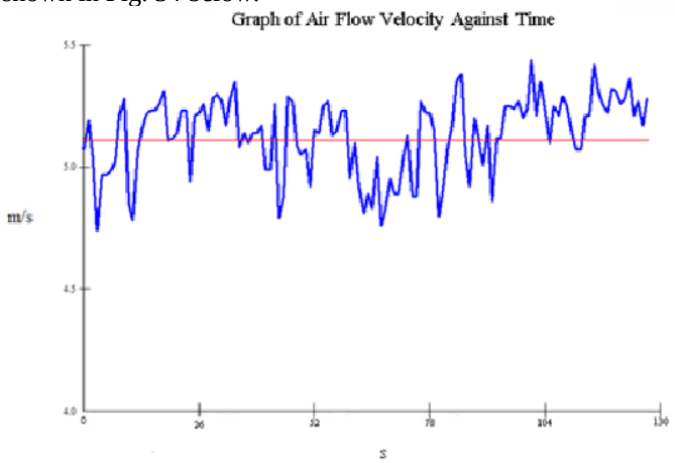

Fig.35. Velocity vs Time for Experiment 1

A CFD simulation as shown in Fig. 36 below was carried out for the wind tunnel to determine velocity inside it.

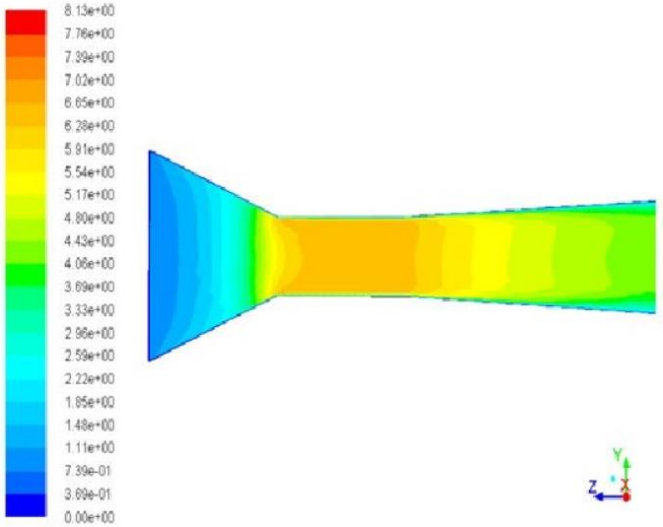

Fig.36. CFD Simulation for Wind Tunnel

A comparison of the results obtained is as shown in Table IV below.

International Journal of Engineering Research & Technology (IJERT)
ISSN: 2278-0181
Vol. 8 Issue 10, October-2019

TABLE IV. EXPERIMENTAL AND SIMULATION RESULTS

Parameter	Experimental Results			CFD Simulation Results
Experiment Number	1	2	3	Overall
Mean Velocity (m/s)	5.12	5.32	5.29	6.28 - 6.65
Turbulence Intensity (%)	3.073	2.055	2.028	2.72 - 3.39

This comparison showed a close agreement between experimental and simulation results. Also, the CFD simulation displayed a greater value of turbulence intensity as compared to experimentation, which was a surprise to the researchers. According to them, it could have been due to the fact that the experimentation exhibited only stream-wise results, whereas the simulation displayed overall turbulence intensity considering longitudinal, transverse and vertical flow. Finally, the researchers concluded that the objective of their project was achieved and small scaled-down test specimen could be tested in the wind tunnel.

VIII. CONCLUSIONS

Wind tunnels are essential tools used for experimentation by experimentalists to accompany analytical and experimental methods. Their design is an iterative process which should discourse a different constraints and requirements. [5]

During the testing of a NACA 2412 airfoil, the blockage ratio increased with the angle of attack and simultaneously the mean fluid velocity decreased in the test section. This caused a reduction in the amount of lift at around 8° of angle of attack. [8]

For obtaining high velocities in the test section, a fan having pointed and sleek two or three blades, placed at the leading end of the wind tunnel can be the choice. Similarly, an exhaust fan with a high H.P. can be used for the same. [2]

Honeycomb structure, if placed before the test section, does not make any difference in lowering the turbulence, but can save time and cost. [2]

For the purpose of fabricating low-speed subsonic wind tunnels, the best suited material for constructing the contraction cone and diffuser is plywood and that for the test section is Plexi glass. [17]

Wind tunnel screens are normally made up of metal wires which are interwoven to make square or rectangular meshes. Nowadays, nylon or polyester is also being used. The variations in longitudinal mean velocity can be minimized to almost zero by using a screen having a pressure drop co-efficient of about 2. [11]

IX. ACKNOWLEDGMENT

We would like to express our sincere thanks and gratitude to all the authors and researchers for their work on design, fabrication and testing of low subsonic open-circuit wind tunnels.

REFERENCES

[1] Andrej Samardzic, Jackson Gillenwaters and Thomas Cieslewski , ‘ Design of Unsteady Wind Tunnel’, Project Thesis of Degree of Bachelor of Science in Aerospace Engineering, Worcester Polytechnic Institute. [Courtesy: NASA]

[2] Mansi Singh, Neha Singh & Sunil Kumar Yadav, “Review of Design and Construction of an Open Circuit Low Speed Wind Tunnel”, Global Journal of Researches in Engineering Mechanical and Mechanics Engineering, Volume 13, Issue 5, Version 1.0, 2013.

[3] Barlow, Jewel B. Rae Jr, William H. Pope Alan. “Low Speed Wind Tunnel Design”, 3rdEdition, John Wiley and Sons Inc. New York, NY, 1999.

[4] R. D. Mehta and P. Bradshaw, “Design rules for small low speed wind tunnels”, Aeronautical Journal November 1979, 443–449.

[5] Louis Cattafesta, Chris Bahr, and Jose Mathew, “Fundamentals of Wind-Tunnel Design”, Encyclopedia of Aerospace Engineering.

[6] John Lohan, “Design and Application of Low Speed Wind Tunnels”, Galway-Mayo Institute of Technology, Galway, Ireland, 2002.

[7] Mehta, R. D., 1977. “The Aerodynamic Design of Blower Tunnels with Wide-Angle Diffusers”. Prog. Aerospace Sci., Vol 18, No. 1, pp 59-120

[8] Peter John Arslanian, Dr. Payam Matin, “Undergraduate research on conceptual design of a wind tunnel for instructional purposes”, American Society for Engineering Education, 2012.

[9] B. Navin Kumar, K.M. Paramasivam, M. Prasanna, A.Z.G. Mohamet Karis, “Computational Fluid Dynamics Analysis of Aerodynamic Characteristics of NACA 4412 vs S809 Arifoil for Wind Turbine Applications”, International Journal of Advanced Engineering Technology, Vol. VII, Issue III, 2016, pp 168-173.

[10] Bapu Joglekar, Rana Manoj Mourya, “Design, Construction and Testing Open Circuit Low Speed Wind Tunnel”, International Journal of Electrical and Electronics Research Vol. 2, Issue 4, pp: (271-285), Month: October - December 2014.

[11] R. D. Mehta and P. Bradshaw, “Design rules for small low speed wind tunnels”, Aeronautical Journal November 1979, 443–449.

[12] Nagendra Kumar Maurya, Manish Maurya, Avdhesh Tyagi, Shashi Prakash Dwivedi, “Design & Fabrication of Low Speed Wind Tunnel and Flow Analysis”, International Journal of Engineering & Technology, 7 (4.39) (2018) 381-387.

[13] Jonathan H. Watmuff, “*Wind Tunnel Contraction Design*” (Proc. of 9th Australasian Fluid Mechanics Conference, Auckland, 1986), pp. 472–475.

[14] Md. Arifuzzaman, Mohammad Mashud, “Design Construction and Performance Test of a Low-Cost Subsonic Wind Tunnel”, IOSR Journal of Engineering (IOSRJEN), Volume 2, Issue 10 (October 2012), PP 83-92.

[15] Vikas Dalal, “Designing and Construction of Low Speed Wind Tunnel WiWu To Investigate the Robustness of Small Model Aircrafts and Launcher Controllers”, Luleå University of Technology Department of Computer Science, Electrical and Space Engineering.

[16] Mauro S, Brusca S., Lanzafame R., Famoso F., Galvagno A. and Messina M., “Small-Scale Open-Circuit Wind Tunnel: Design Criteria, Construction and Calibration”, International Journal of Applied Engineering Research ISSN 0973-4562 Volume 12, Number 23 (2017) pp. 13649-13662.

[17] T.H. Yong and S.S. Dol, “Design and Development of Low-Cost Wind Tunnel for Educational Purpose”, IOP Conference Series: Materials Science and Engineering, 2015.